Supporting Information

New insight on optical and magnetic Fe_3O_4 nanoclusters promising for near infrared theranostic applications.

Chih-Chia Huang [a,b,c*] *Po-Yang Chang,* [a,b] *Chien-Liang Liu,* [a] *Jia-Pu Xu,* [b] *Shu-Pao Wu,* [d] *and Wen-Chuan Kuo,* [b,c*]

[a] Department of Photonics, Center for Micro/Nano Science and Technology, and Advanced Optoelectronic Technology Center, National Cheng Kung University, 701, Tainan, Taiwan.
[b] Institute of Biophotonics, National Yang-Ming University, Taipei, 112, Taiwan.
[c] Biophotonics and Molecular Imaging Research Center (BMIRC), National Yang-Ming University, Taipei, 112, Taiwan
[d] Department of Applied Chemistry, National Chiao Tung University, Hsinchu, Taiwan.

Email: c2huang@mail.ncku.edu ; wckuo@ym.edu.tw

To study in vitro release, we incubated FITC-absorbed Fe_3O_4 CNPs (1000 $ppm_{[Fe]}$) in phosphate-buffered saline (PBS) buffer solution (1 mL) at different aging time. The loss of FITC was carefully collected and quantified to estimate the residual amount of FITC (0.75 μM) within Fe_3O_4 CNPs (1000 $ppm_{[Fe]}$). Although the interaction between FITC molecule and the surface of Fe_3O_4 CNPs is followed with physical absorption, the FITC leakage after 14 days was negligible when compared to the loading FITC molecule at the same concentration. This result indicated that the release of FITC would be depleted for any interference in the confocal imaging of HeLa cells incubated with FITC-absorbed Fe_3O_4 CNPs (4h).

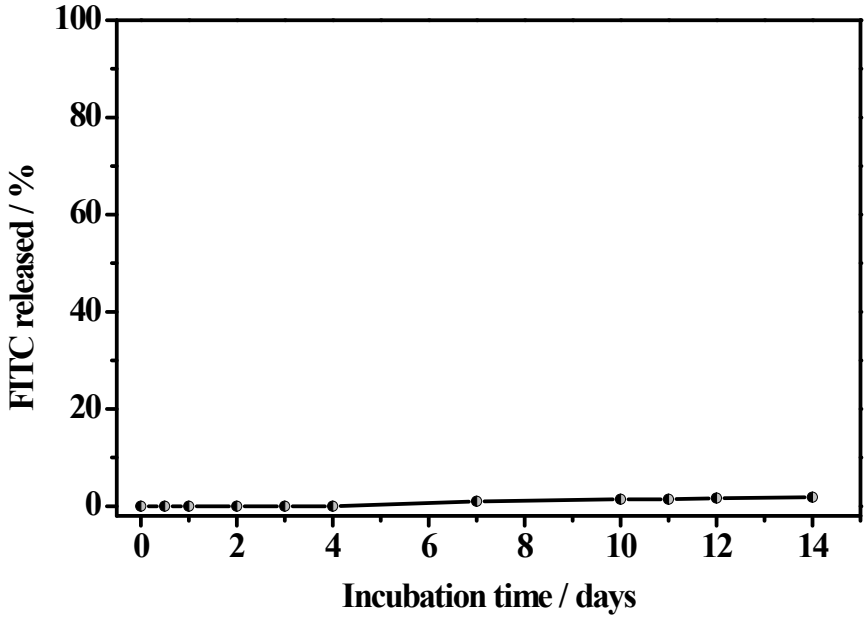

Figure S1. In vitro release profile of FITC molecule from FITC-absorbed Fe_3O_4 CNP solution at 37 ^oC

Figure S2 shows optical analyses of the as-obtained Fe_3O_4 CNPs to identify the carboxylate molecules at the surface. The assignments were according to the literature.[1-4] Figure S2a shows a FT-IR spectrum. A band at 570 cm^{-1} appeared, which is consistent with the Fe–O vibrations of the Fe_3O_4 structure. The absorptions at 1558 and 1373 cm^{-1} are assigned to the carboxylate groups of νas(COO)- and νs(COO)-, respectively. The peak labeled f at 1745 cm^{-1} could be attributed to free –COOH. A surface analysis using X-ray photoelectron spectroscopy (XPS) (Figure S2b-d, Supporting Information) determined the Fe 2p oxidation state at 710.1 eV ($2p_{3/2}$) and ~723.5 eV ($2p_{1/2}$) matching the Fe2+/3+ ions in the Fe_3O_4 CNPs. The O 1s spectrum presented a band at approximately 539.5 eV, in agreement with the lattice O^{2-} of the Fe_3O_4. The additional broadening of the band obtained at ~531.5 eV can be ascribed to the Fe-O complex at the surface and exposed COOH, C=O, and –OH groups from the binding TMA/citrate molecules. A signal at 284.3 eV was calibrated using the C1s photoelectron peak. Peaks at 286.4 eV and 289 eV are due to the organic ligand coating layer on the particle surface.

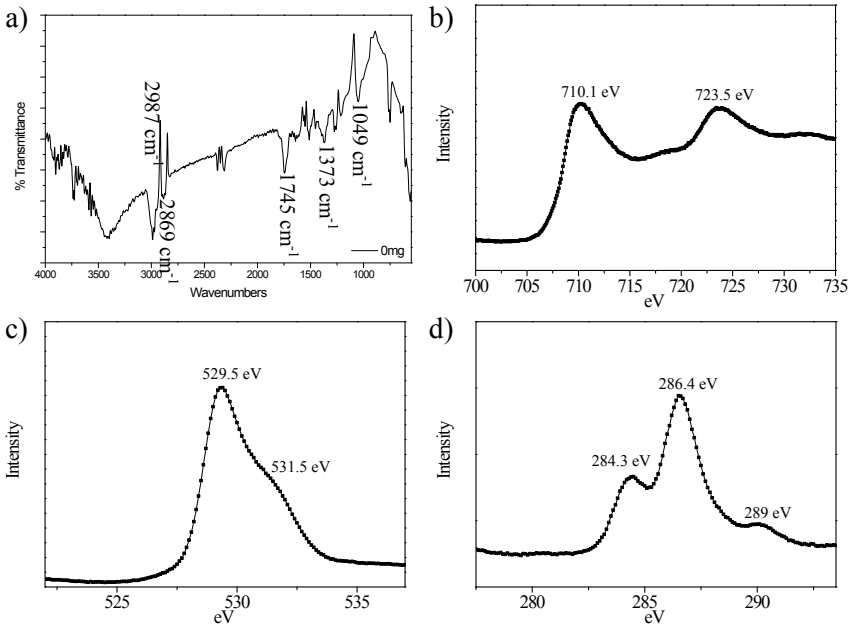

Figure S2. a) FT-IR measurement of as-prepared Fe_3O_4 CNPs. High-resolution XPS core-level spectra of b) Fe 2p, c) O 1s, and d) C 1s for as-prepared Fe_3O_4 CNPs.

[1] A. G. Roca, J. F. Marco, M. d. P. Morales, C. J. Serna, *J. Phys. Chem. C* **2007**, *111*, 18577.

[2] M. Y. Liao, C. H. Wu, P. S. Lai, J. S. Yu, H. P. Lin, T. M. Liu, C. C. Huang, *Adv. Funct. Mater.* **2013**, *23*, 2044.

[3] M.-Y. Liao, P.-S. Lai, H.-P. Yu, H.-P. Lin, C.-C. Huang, *Chem. Commun.* **2012**, *48*, 5319.

[4] Y.-L. Huang, H.-W. Tien, C.-C. M. Ma, S.-Y. Yang, S.-Y. Wu, H.-Y. Liu, Y.-W. Mai, *J. Mater. Chem.* **2011**, *21*, 18236.

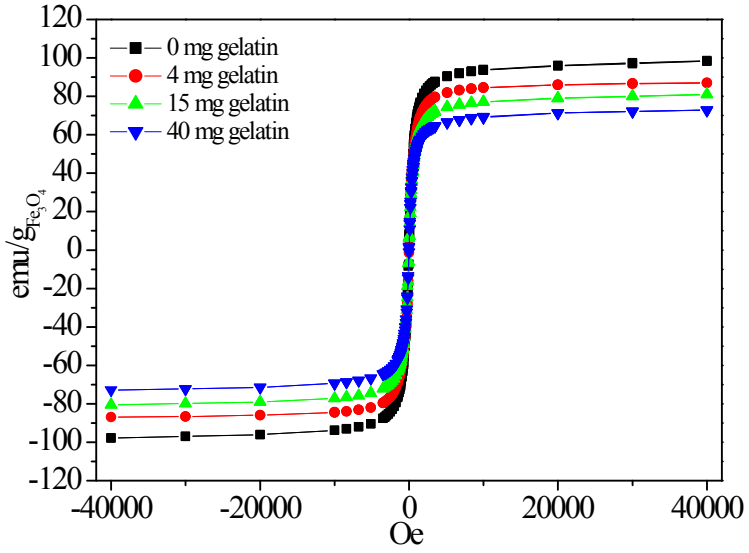

FigureS3. SQUID measurements of the M-H curves (300 K) for the as-prepared Fe_3O_4 CNPs after the hydrothermal reactions (200 ^oC and 13 h) of $FeCl_2$, citrate ions, TMA, and N_2H_4 with different concentrations of gelatin molecules.

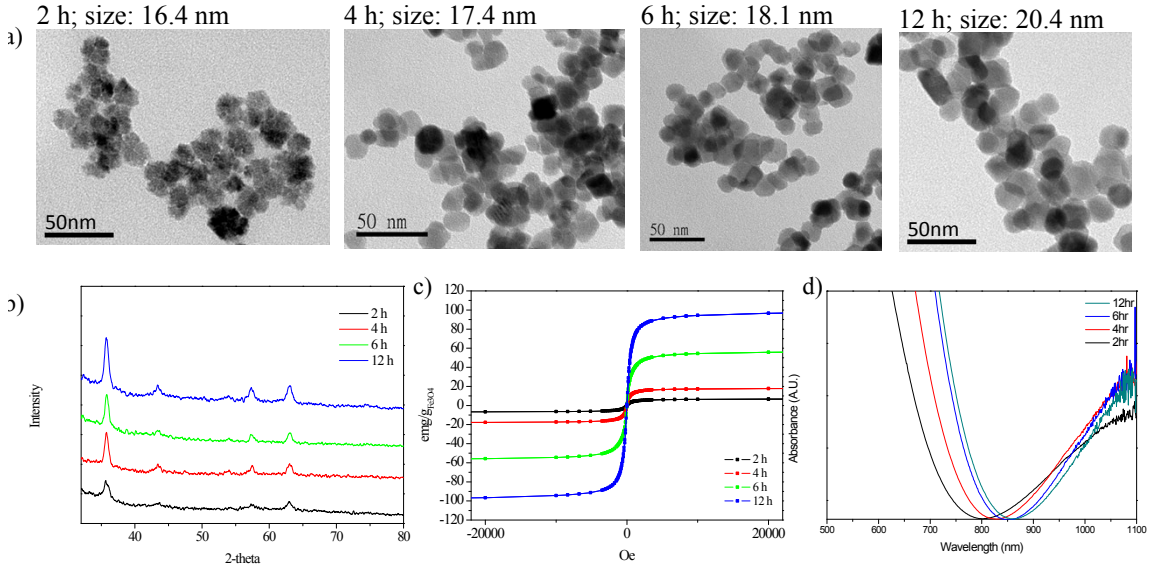

Figure S4. Time-dependent a) TEM images, b) XRD measurements, c)SQUID analysis and d)UV-visible-NIR spectra for monitoring the growth of Fe_3O_4 CNPs.

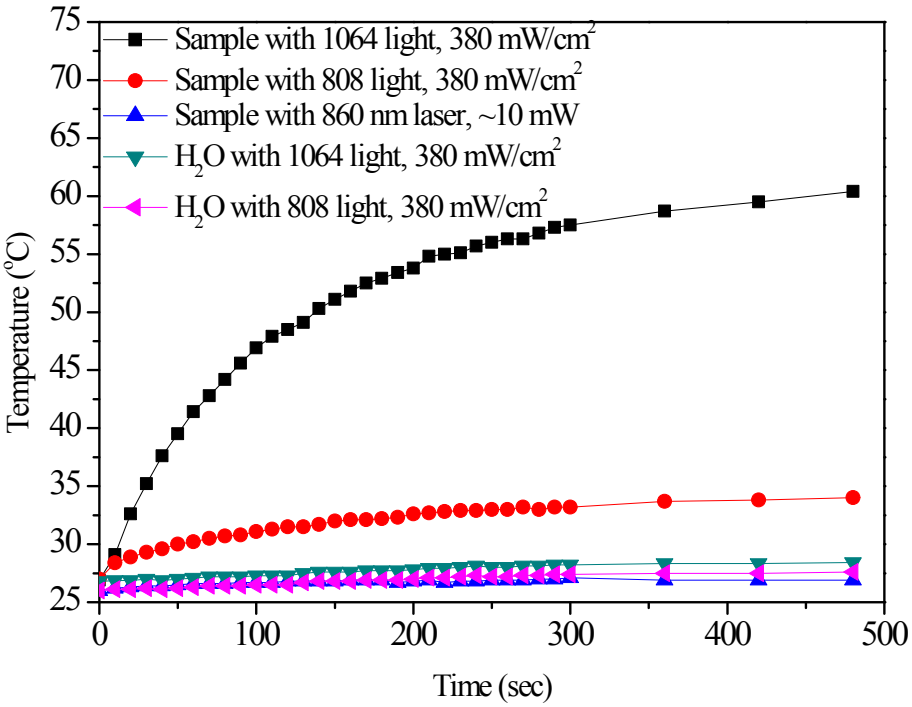

Figure S5. Temperature dependence of the aqueous Fe_3O_4 CNP (375 ppm) solution as a function of laser (NIR-I 808 nm, NIR-I 860 nm (OCT light source), and NIR-II 1064 nm (photothermal light source)) irradiation time.

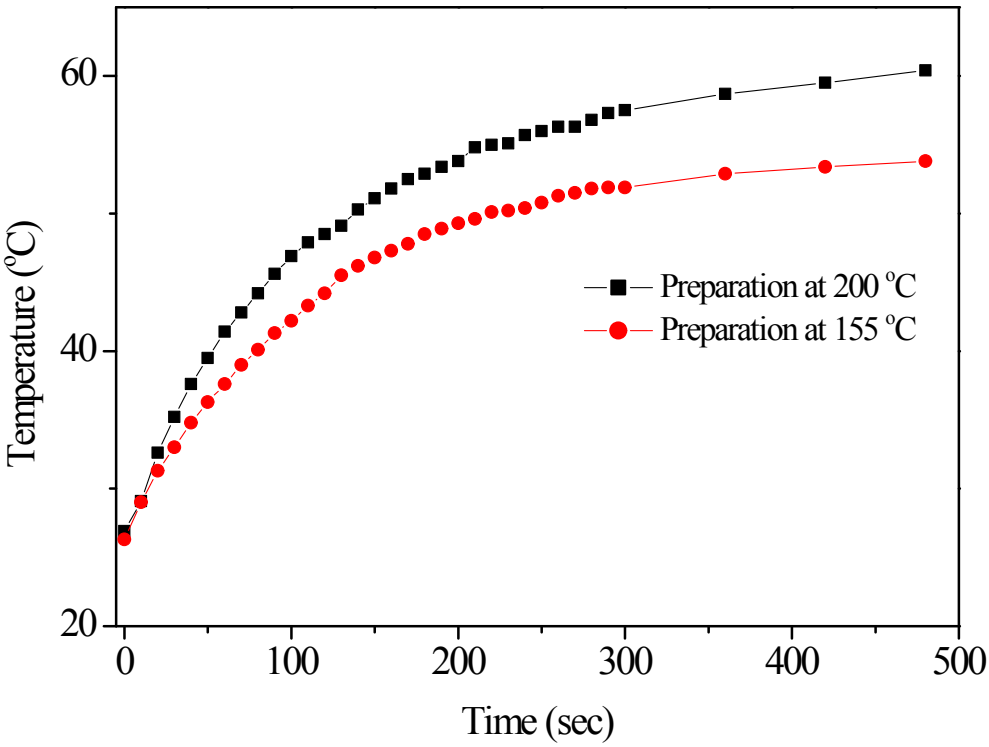

Figure S6. Temperature dependence of the aqueous Fe_3O_4 CNP solution, prepared at 155 °C and 200 °C, as a function of NIR-II laser irradiation at 1064 nm.

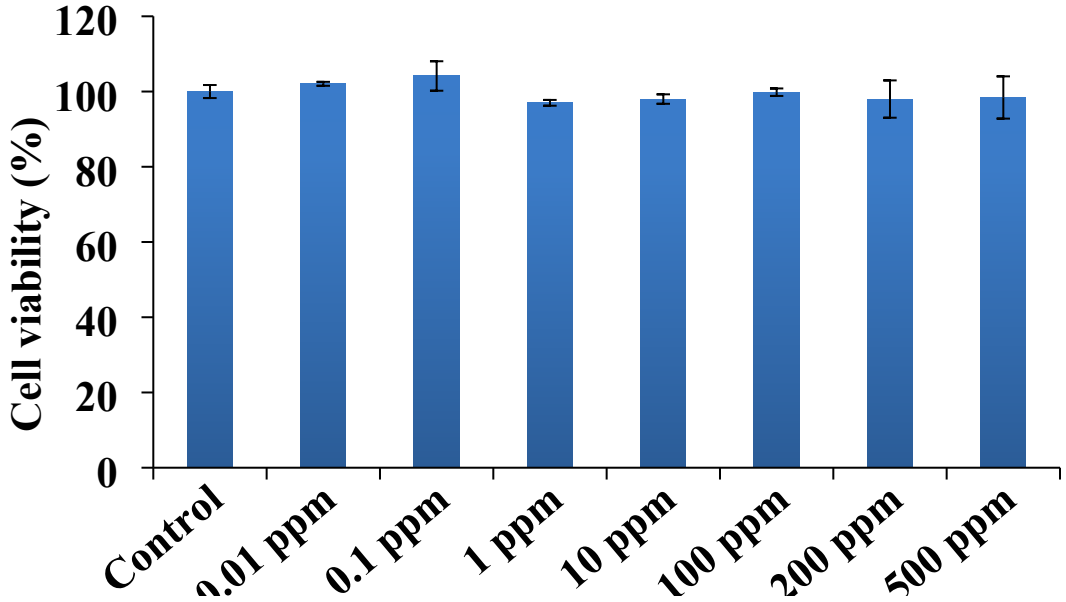

Figure S7. MTT assay of the HeLa cells incubated with Fe_3O_4 CNPs after 24 h.

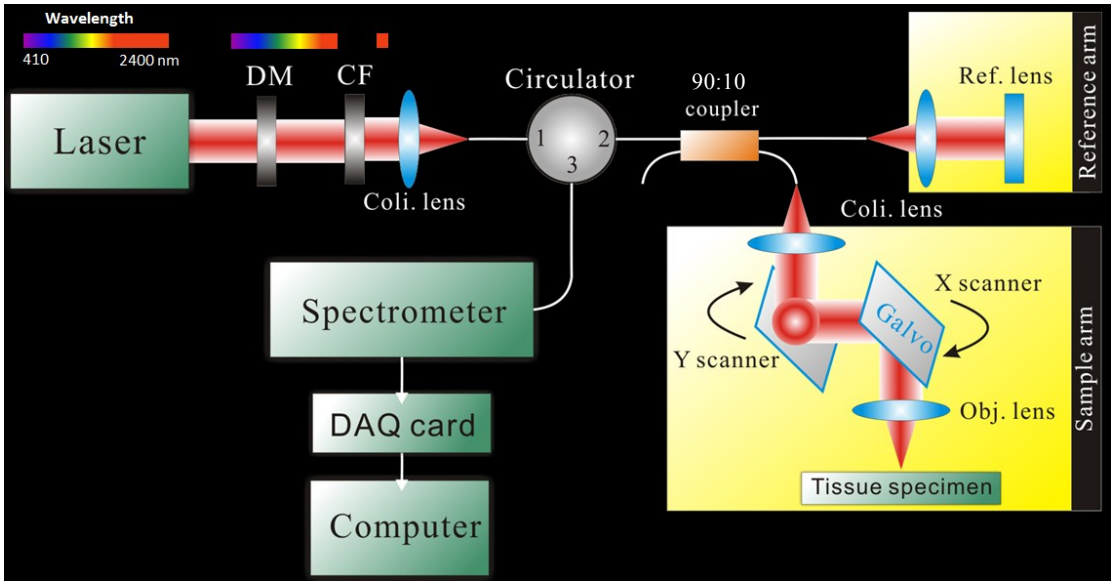

Figure S8. Schematic of the UHR-SDOCT system. Coli. lens: collimation lens, Ref. lens: reference lens mirror, DM: dichroic mirror, CF: color filter, Obj. lens: objective lens, Galvo: galvanometer scanner, DAQ: data acquisition card.

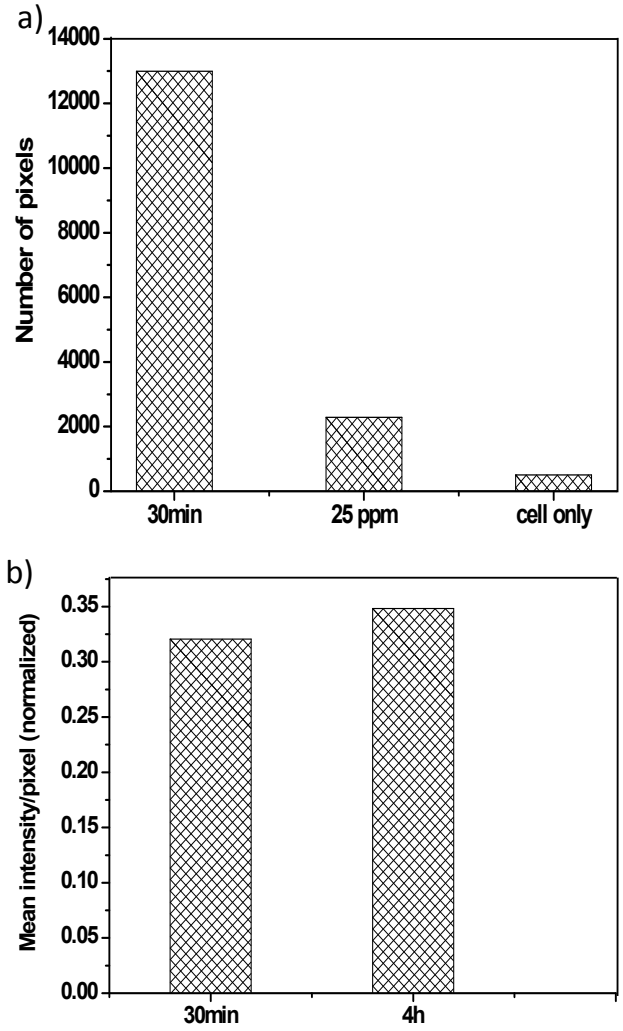

Figure S9. a) Quantitative analysis of the HeLa cells incubated without and with Fe_3O_4 CNPs (150 ppm). b) Analysis of mean intensity per pixel from the HeLa cells (2.4 x 10^5) treated with Fe_3O_4 CNPs (150 ppm) after 30 min and 4 h. The raw data showing the image signals are in Figure 4 and Figure 5 in the main text.

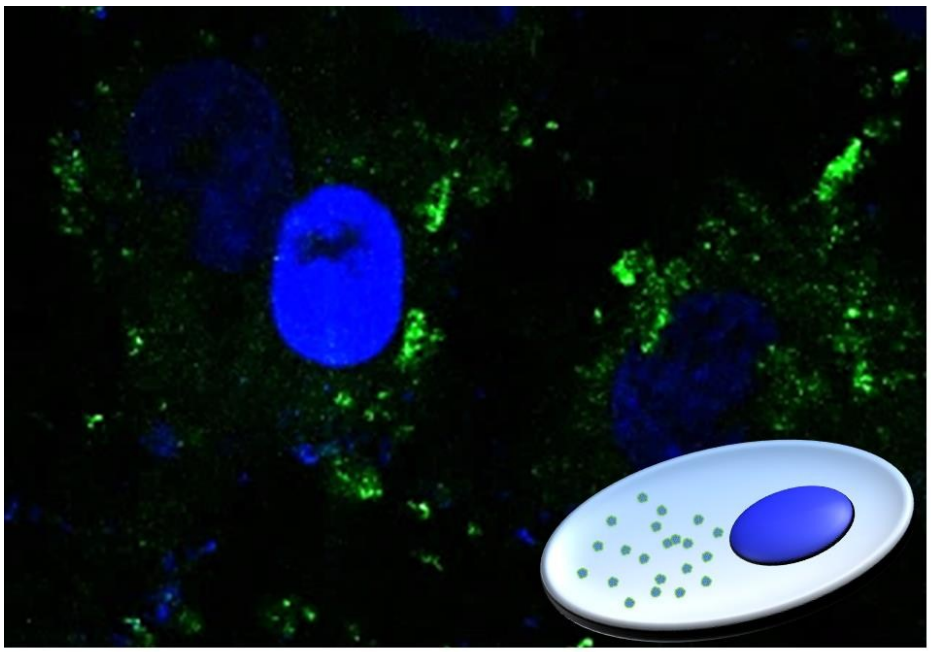

Figure S10. Confocal laser images of HeLa cells treated with FITC-absorbed Fe_3O_4 CNPs CNPs for 4 h. The blue color represents DAPI stained nuclei.

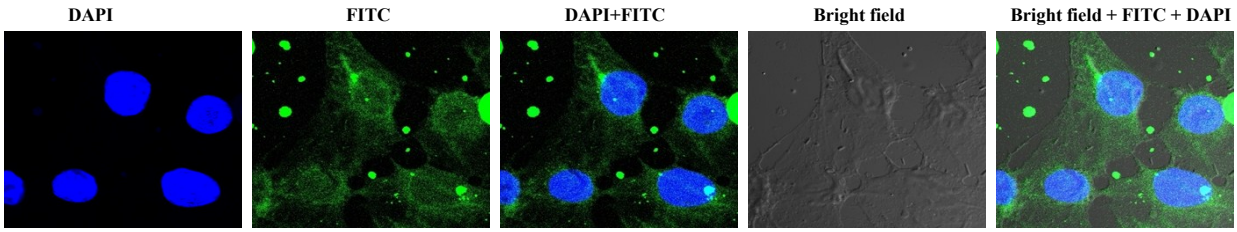

Figure S11. Confocal laser images of HeLa cells treated with FITC alone (green fluorescence) for 4 h. The blue color represents DAPI stained nuclei.

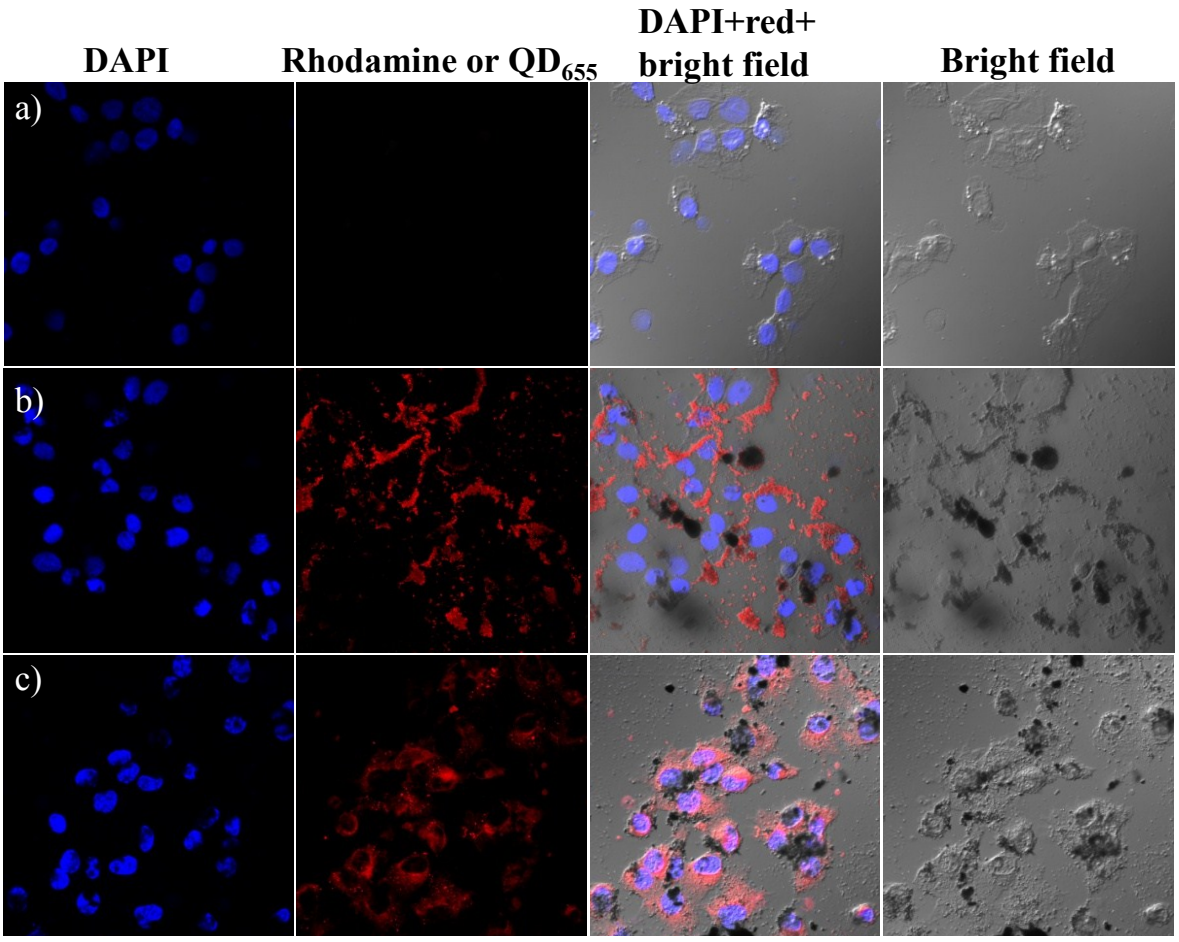

Figure 12. Confocal images of HeLa cells after different treatments: a) cell alone (4 h), b) QD_{655}-conjugated Fe_3O_4 CNPs (4h), and c) Fe_3O_4 CNPs (4 h) + rhodamine-based chemosensor/HCl.

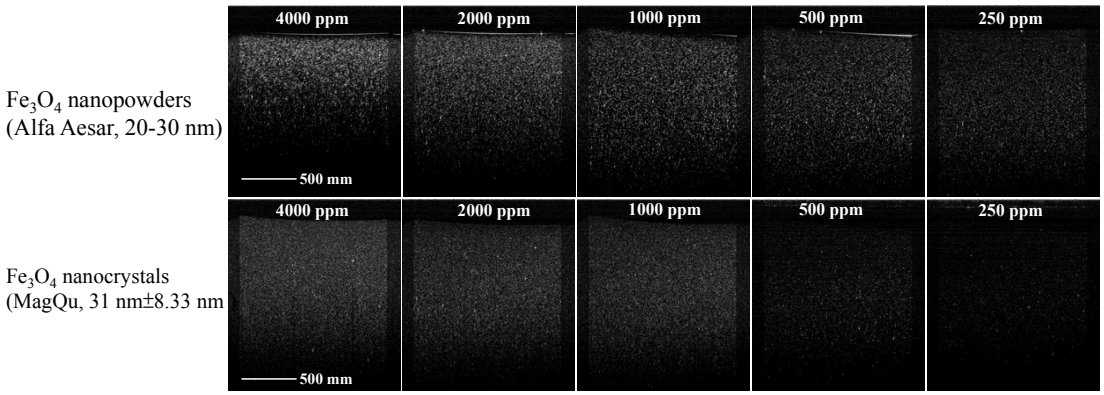

Figure S13. X–Z images from a chamber containing different concentrations of a-e) Fe_3O_4 nanopowder (Alfa Aesar, 20-30 nm) and colloidal Fe_3O_4 nanocrystals (MagQu, 31 nm±8.33 nm) using an OCT microscope system with a laser light source with an 860 nm center wavelength.